Time Domain Spectroscopy Techniques for Non Destructive Contact less Flaw Detection and Imaging in Advanced Materials

J. BECKMANN, J. DÖRING, J. BARTUSCH, U.ZSCHERPEL, U. EWERT, A. ERHARD
Federal Institute for Materials Research and Testing, Berlin, Germany

Abstract. The low electron density of polymers, ceramics and organic materials makes detection of flaws difficult using radiographic methods. Conventional ultrasonic techniques are limited by the necessity to employ coupling media. Airborne ultrasonic at the frequency range of 0.5 MHz - 1 MHz as well as electromagnetic waves between 0.1 THz - 2 THz are emerging technologies that will probably have broad applications for quantitative evaluations of flaws in polymer materials and composites in the next future. The poster explains the similarities and differences of both pulse transducer techniques and the use of data for imaging application to improve flaw detection in step wedges with flat bottom indicators. Image examples for non destructive inspections will be shown.

Introduction

By using time domain spectroscopy (TDS) procedures, air coupled ultrasound (ACUS) techniques as well as pulsed THz radiation systems became a powerful tool for both, the contactless, nondestructiv detection of e.g. flaws and the material characterisation. The two different measurement systems base generally on the interaction of pulses with matter. While the dielectric properties of the sample change the transmitting electromagnetic THz-wave, ultrasound is influenced by the mechanical properties of the material. There exist some specifics in ultrasound technique with air as coupling medium and in THz TDS diagnostic. ACUS and THZ TDS can operate in two different ways, the pulse-echo or the through-transmission mode [1]. In both cases the amplitude and the delay time will be measured, analysed and stored on a PC during a scanning procedure of a test object. Usually, the data are subsequently mapped pixel by pixel to images. Like in the radiographic technique, amplitude (C-scan), delay time (D-scans) or mechanical property images of the object under test can be generated, analysed and evaluated. ACUS advanced and expanded its capabilities in the last decades up to a level that made the development of reliable and safe investigation systems for industrial, medical and security applications possible [2]. On the other side, recent developments in the field of femtosecond (fs) laser and low temperature grown GaAs have culminate in operating THz TDS systems, equipped with photoconductive antennas which are able to emit bright coherent, broadband THz pulses. A coherent THz system makes the time resolved amplitude record of the transmitted or reflected electrical field possible. Like in case of ACUS, technical advance has led to the development of THz imaging systems which can use different parameters of the electromagnetic pulse wave for the material characterisation and flaw detection as well. Nowadays, THz TDS systems are enabled for operating at room temperature. They are considered to have many potential applications in medicine [3], for security applications [4]

and in aircraft and space industry [5]. Images has been produced to check the capabilities of the THz-diagnostic system “T-RayTM 2000” [6] and the ACUS system "USPC 4000 AirTech Hillger" [7, 8] respectively. The presented results document the examinations on step wedges with integrated flat bottom and drill through holes. The step wedges were machined from polyethylene (PE) and polyvinylchlorine (PVC) plates. Additional, x-ray radiographs of the wedges has been produced to demonstrate the complementarities of the different imaging tools

1. Experimental: Generation of measurement pulses

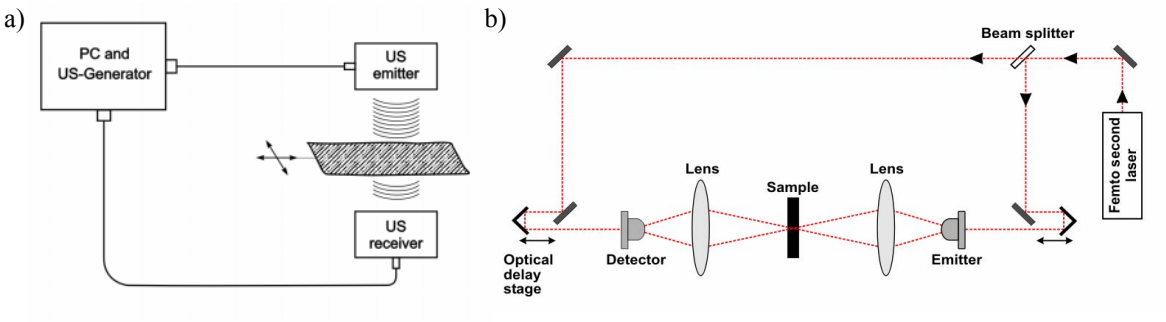

Fig. 01: Schematic diagram of the set up of transmission type TDS system
a) air coupled ultrasound system (ACUS); **b)** THz TDS imaging (TIS)

Fig. 01 shows schematically the experimental setup for the imaging experiments on step wedges in the transmission mode. As documented in Fig. 01a, the ultrasonic experiment is equipped with a self constructed x – y – stepper motor translation stage, a programmable generator and two transducers, acting as ultrasonic emitter and receiver respectively. First the "ULTRAN GN-55" sensors [9] have been elected as transducers.

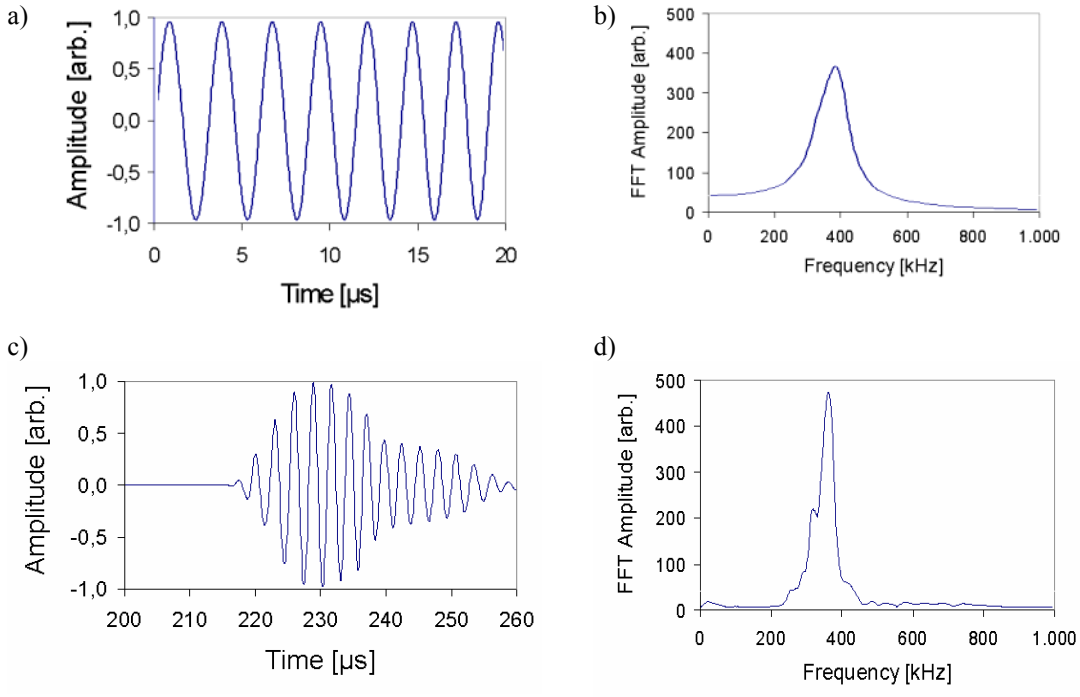

Fig. 02: Signal of "ULTRAN GN-55" driven by a programmable pulse generator
a) programmed burst; **b)** Fourier transformed burst with centre frequency and bandwidth;
c) received acoustic signal; **d)** and its amplitude spectrum

They consist of composite material and are equipped with λ/4-layers for matching the acoustical impedance of the composite and air. The λ/4-layers reduce the reflection coefficient and subsequently the attenuation. Unfortunately the λ/4-layers cause an extension of the pulse and a shortening of the frequency bandwidth too. In an ACUS system, a programmable generator drives the sound emitting ULTRAN GN-55 sensor by sinusoidal voltage wave packages (bursts) (s. Fig. 02a, 02b). The pulse response of the sensors is matched by the election of the driving burst centre frequency and band width (Fig. 2b). The shape and amplitude differences between the programmed theoretical pulse (Fig.02a, 02b) and the received acoustic pulse (Fig.02c, 02d) are caused by the UT-generator and the pulse response of the transducer themselves.

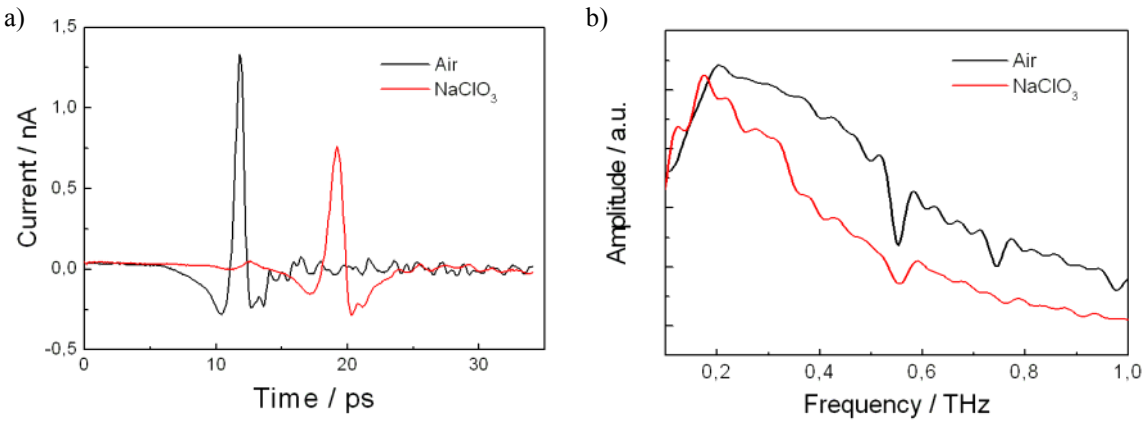

Fig. 03: Waveform of measured terahertz pulse transmitted through air and $NaClO_3$ **(a)** and their spectrum **(b)** (measured at the TU Braunschweig Institut für Hochfrequenztechnik, Germany from A. Kupsch).

A transmission type THz TDS imaging system (TIS) is constructed in a more complicated way, but basically not different from an ACUS. As illustrated in Fig. 01b the TIS uses two photoconductive antennas for the generation and the detection of THz pulses. The heart of the system is an ultra-short femtosecond Ti:Sapphire laser which produces pulses of about ~ 100 fs duration time and wavelength typically centred at about 780 nm. The pulse train beam is splitted into a pump and a probe beam. The pump beam is directed onto a semiconducting THz generator (emitter antenna) which converts the pulses in THz pulses. Further, the THz radiation is collected and focused by a HDPE or Silicon lens pair system onto the sample. The transmitted THz radiation is detected by a second semiconducting antenna, which is triggered by the probe beam. The amplitude of the THz pulse is measured by optically gating the receiver and measuring the current flow driven by the instantaneous voltage of the transmitted electrical THz field. The complete time resolved electrical field amplitude is collected by varying the optical path length of the probe beam via a motor controlled delay stage. A typical time dependency of amplitudes (waveforms) of the electric THz pulses, which are transmitted through air and $NaClO_3$ are shown in Fig. 03.

2. Transmission Imaging

The imaging studies were performed on different step wedges. The initial work conducted was to investigate the effects of the different methods on the image quality. Fig. 04 shows the photograph of a PVC step wedge, its radiograph and the corresponding THz images containing the maximum amplitude of the pulse height and the delays in the time domain respectively. Fig. 05 depicts the technical graph of a flat bottom PE step wedge, the magnitude THz TDS image of a step wedge region as well as the photograph of step wedge implemented in the ACUS experiment.

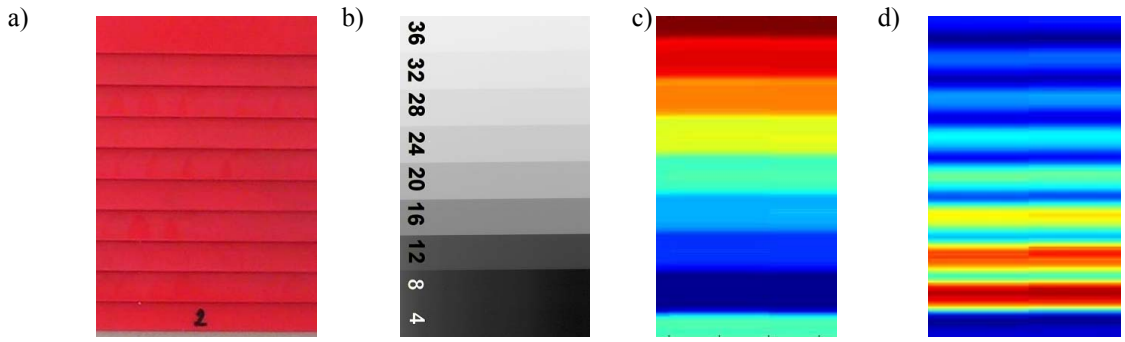

Fig. 04: Images of a PVC step wedge ranging from 4 to 36 mm and having a step size of 2 mm;
a) photograph; **b)** radiograph, U= 16 kV; I= 8 mA; t= 1 min; FFA = 700 mm; AGFA D4 (C3)
TIS: **c)** peak to peak measured time delay of THz pulse; **d)** maximum amplitude image of THz pulse.

Fig. 06a and Fig. 06b show the imaging results gathered from the transmission ACUS experiments of the step wedge which has been detailed described in Fig. 05a. The magnitude and delay time measurement indicate the same signal behaviour as observed in the case of THz TDS experiments.

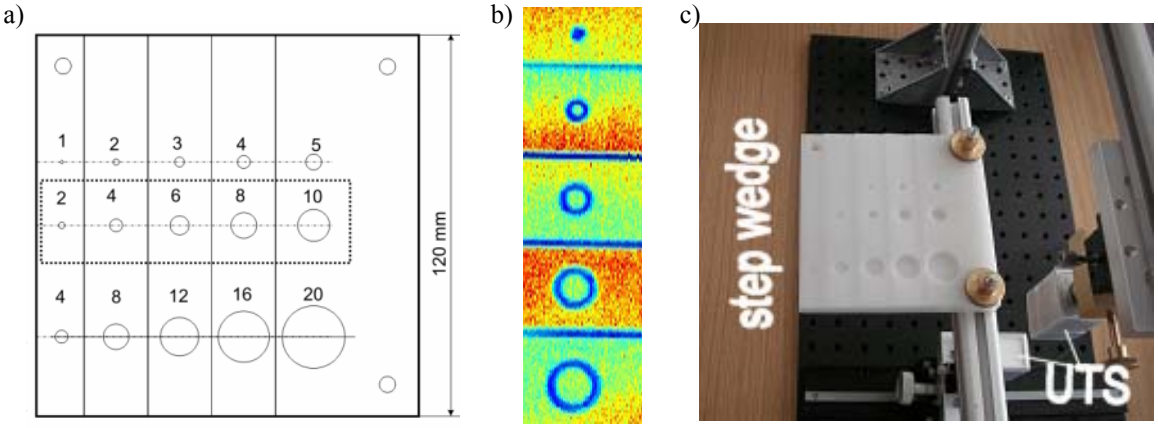

Fig. 05: Flat bottom PE step wedge (ranging from 10 to 15 mm and a step size of 1 mm);
a) Technical graph, the numbers inside the step describe the diameter of the flat bottoms; the depths of the holes are indicated by the numbers of the topmost row. **b)** THz imaging, scanning area is marked by the dotted points in the graph (Fig. 05a); the magnitude indicates the integral over a frequency band form 1 to 2 THz. **c)** Experimental set up of ASCUS with step wedge and ultrasonic sensors (UTS.)

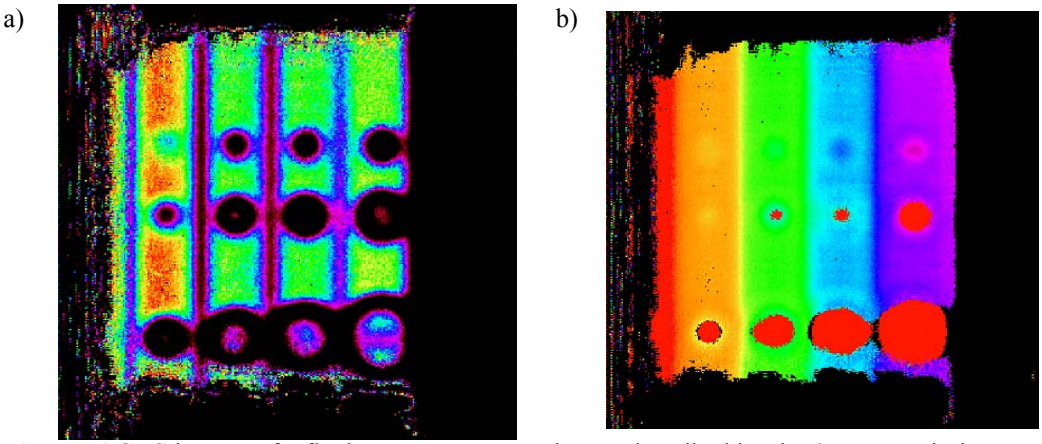

Fig. 06: ACUS images of a flat bottom PE step wedge, as described in Fig. 05a transmission measurement with pulse compression:
a) maximum amplitude of pulse in time domain (C-scan) and **b)** delay time (D-scan).

Fig. 06a and Fig. 06b show the imaging results gathered from the transmission ACUS experiments of the step wedge which has been detailed described in Fig. 05a. The magnitude and delay time measurement indicate the same signal behaviour as observed in the case of THz TDS experiments. The sharp edges located at the holes and steps cause a reduction of the signal intensity due to scattering and deflection of the sound. Further, in a transmission situation, the airborne ultrasound signal traverses through both sample sides. The pulse passes an air – material transition and vice versa before it is reached by the receiving transducer. Thereby the transmitted pulses are strongly weakened by reflections and subsequently, signals with considerable low signal to noise ratio can only be detected and analyzed. A pulse compression technique is known to improve the signal quality essentially [10]. The technique correlates the received signals measured without and with the sample. Normally, the cross-correlated signal posses a pulse amplitude maximum to noise ratio that is much higher than that of the originally measured one. Thus, the magnitude image appears less noisy and has a better contrast as shown in Fig. 06a. Interestingly, pulse compression is also improving the imaging quality of the delay time in Fig. 06b. The signal compression technique is universal and can be applied for THz-TDS imaging as well.

3. Pulse Echo Imaging - Technique for Determination of the Shape of a Component

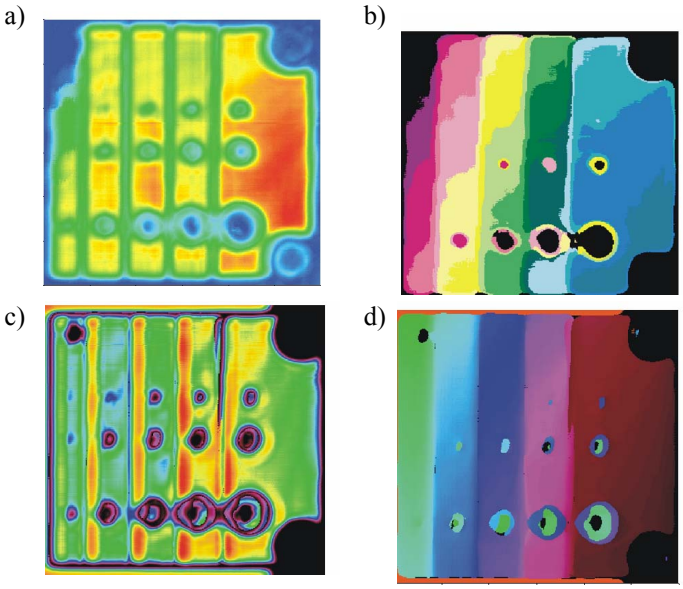

Fig.07: Pulse echo measurement
a) C-scan; **b)** D-scan; **c)** C-scan with pulse compression;
d) D-scan with pulse compression;

Short ultrasonic pulses generated by a transducer to travel through thick material ($\lambda \ll d$) are partially reflected to the original transducer from the surface, back and discontinuities of the sample. The so called pulse-echo technique basically locates the discontinuities or material thicknesses by accurately measuring the travelling time of the reflected ultrasonic pulses. Fig. 07a and Fig. 07b show the pulse echo images of the C- and D-Scan calculated from the online gathered data. The Fig. 07a and Fig.07c, i.e. the C-scans, yields the reflectivity of the surface and the shape of the surface can be measured with the D-scans (Fig. 07b and Fig. 07d). The image quality could be improved and more details be seen, after the pulse compression technique has been applied (Fig. 07c and Fig. 07d). In contradiction to Fig.07a the upper line of the flat bottom holes appears on the improved image in Fig.07c. Additionally, the whole data set of the volume scan has been used to construct a three dimensional view of the above described PE step wedge with embedded flat bottom holes. Fig.08 depicts the 3D view of the step wedge with steps, flat bottom holes und the bottoms of the holes in detail. Besides the shape coloured coded information is shown in the graph. The colours represent the amount of the reflected pulse amplitude at that receiver position. Thus, beside the depth resolution information about the surface texture can be gained from the reflected pulse as well.

Fig. 08 shows, that in contradiction to the transmission experiment, the pulse-echo technique can conserve the depth information in the received signal. The stored delay time data allow the complete reconstruction of the test object shape and the locale position of flaws.

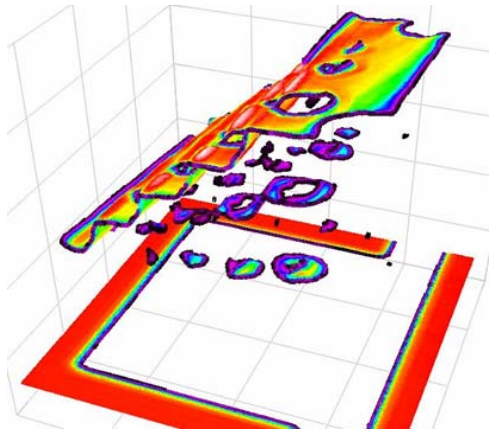

Fig.08: 3D Texture of the step wedge (Fig. 06)

In comparison to the transmission experiment the pulse-echo technique is considered to be the more preferred method because it requires only a one side access and can provide the sample texture and surface properties by simultaneous measurements of the delay time and amplitude of the reflected pulse. Generally, the considerable large ratio of the acoustic impedances of solids to air induces high sound attenuations what is considered to be the main problem of ACUS. The impedance matching problem is still present in the field of transducer developments. Two possibilities could be observed to enhance the transducer efficiencies.

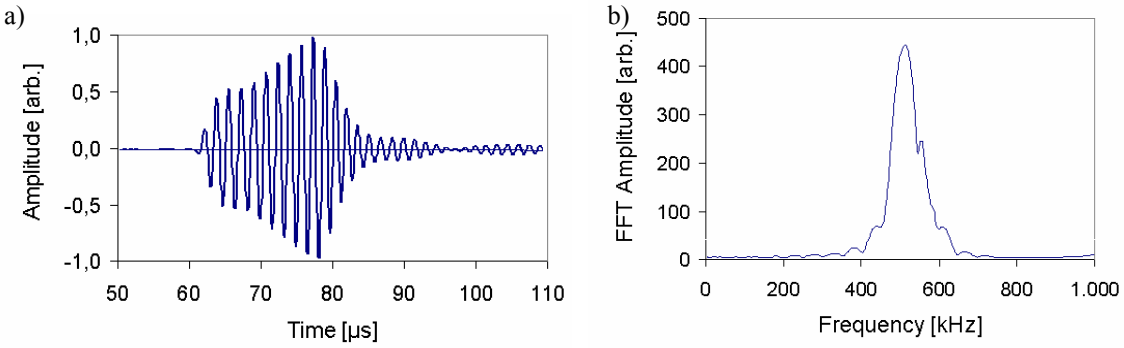

Fig. 09: Signal **(a)** of an EMFI transducer, received after reflection and its amplitude spectrum **(b)**.

.

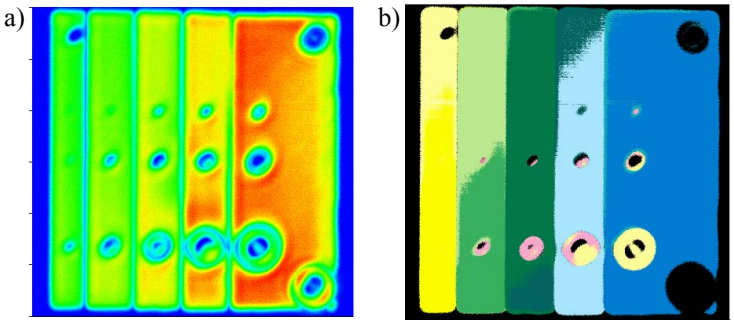

Fig. 10: Scan of the step wedge with a EMFI transducer
(a) amplitude (C-scan) and **(b)** delay time (D-scan)

Firstly, the improved acoustic impedances matching by adding λ/4-layers, as demonstrated by "ULTRAN GN-55" sensors [9] have been described. Secondly, the reduction of the reflection loss at the transducer - air - interface using polypropylene foam foils as active element, which have a lower acoustic impedance than the solid material [11, 12]. As already describe for the ULTRAN GN-55 sensor the programmable generator produces appropriate bursts for the transducer. The received test pulses of the last described prototype transducer, the so-called EMFI transducer is shown in Fig. 09a. The Fourier transformation in Fig. 09b defines the signal with a centre frequency of 510 kHz. A C- and a D-scan of the step wedge registered with an EMFI transducer are shown in Fig. 10a and Fig. 10b. In spite of the less sensitivity and the less complex construction of the transducer the images show a good SNR comparable to the ULTRAN sensor (Fig. 07a – Fig. 07d).

4. Discussion

Material analysis by means of transmitting millimetre waves as well as transmitting acoustic waves can be expressed by the same solution (equation 1) of the wave equation for a wave, travelling in the z direction in isotropic medium.

$$u^*(z,t) = u_0 \exp\{j(k^* z - \omega t)\} \qquad (1)$$

u – amplitude of travelling wave varying sinusoidally in both space and time
k* - complex wave number; ω- angular frequency; t - time.
For a plan acoustic wave, equation (1) can be modified to

$$u^*(z,t) = u_0(t)^* \exp\left\{ j\frac{\omega}{v_L} \right\} \exp\{-\alpha z\} \qquad (2)$$

u – is the translation in propagation direction z;
The experimental estimation of the longitudinal sound velocity v_L and the attenuation coefficient α for the material under test allows the calculation of its complex longitudinal modulus L(ω)* = L' + jL according to equation (3).

$$L' = \rho v_L^2, \quad L'' = 2\rho v_L^3 \alpha_L / \omega, \qquad (3)$$

The delay time t has to be determined for an exact calculation of the material parameters v_L or L' . Usually, the density ρ is separately estimated.
In case of a plane electromagnetic wave arranged perpendicular to the propagation direction z, following equation (5) can be expressed by means of the complex refraction index (equation 4).

$$\hat{n} = n - jn\kappa \qquad (4)$$

n – refraction index is defined by the ration of the phase velocities of the electromagnetic wave in vacuum (light velocity c) to matter c_m; κ - absorption index.

$$E^*(z,t) = E_0(t)^* \exp\left\{ j\frac{n}{c} \right\} \exp\left\{ -\frac{\omega}{c} n\kappa z \right\} \qquad (5)$$

The imaginary part of equation (4) effects a real exponential function in equation (5) which describes an attenuation of the electrical field in the isotropic medium. The attenuation factor can be simplified to exp(-2πκz/λ) (λ – wave length). The real and imaginary part of the complex refraction index of a sample with known thickness can be estimated experimentally due to transmission experiments. The complex dielectric properties of the sample can be subsequently determined by equation (6)

$$\varepsilon\mu = n^2(1-\kappa^2); \qquad \sigma\mu = 2\varepsilon_0 \omega n^2 \kappa \qquad (6)$$

ε - dielectrical permittivity; μ - magnetic permeability; σ - current conductivity.
The offline line calculation of the material properties from the experimental ACUS data has shown difficulties because the delay time of a pulse or between two pulses could not measured exactly enough if the pulses have more than one wavelength. This problem has been solved by using the mentioned pulse compression with the cross-correlation technique. The calculated cross-correlation maximum could very exactly determine the time position of the delay time difference of the correlating signals as already reported in the literature [13]. To demonstrate the advantage of the described technique, we have used the basic configuration of the ACUS system "USPC 4000 AirTech Hillger", and performed a volume scan of the described PE step wedge in pulse-echo-technique.

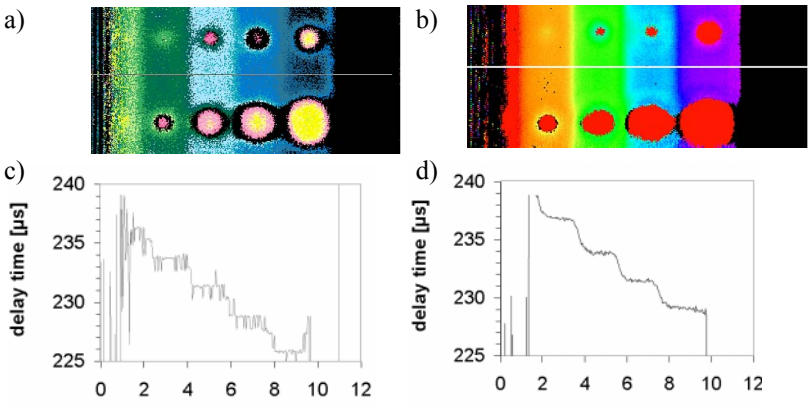

Fig.12: Delay time measured in transmission mode (Ultran sensors),
a) D-Scan without compression; **b)** D-Scan with pulse compression
c) Profile plot of from Fig.12a; **d)** Profile plot from Fig.12b.

An emitter - receiver distance 8…9 cm has been used for a reference signal. A transducer device distance of about 4 cm has been selected for the scanning. Both amplitude (C-Scan) and delay time (D-scan) has been extracted from the raw data imaging scan and are already shown in Fig. 06.The profile plots of the images of Fig. 11 demonstrate the improved signal to noise ratio by pulse compression. Based on the improved profile plot of the step wedge a sound velocity of PE can be calculated on the base of the relative delay time values, shown in Fig. 12b and the measured step size x. Then sound velocity of this material (PE) is: $v_{mat} = (x_1-x_2) / ((t_1-t_2) + (x_1-x_2)/v_{luft}) = 3,1 / (-7,7 + 3,1/0,344) = 2,36$ km/s .

Summary

Time THz radiation systems (THz-TDS) and airborne ultrasonic systems (ACUS) can detect the shape and the material properties of a polymer component at the same time by using the time domain spectroscopy technique. The results of each complementary system can be composed to a more complete image of the sample under test.

References

[1] J. Krautkrämer, H. Krautkrämer „Werkstoffprüfung mit Ultraschall“, Berlin, Springer, 1986,
[2] M. C. Bhardwaj, "Non-Destructive Evaluation: Introduction of Non-Contact Ultrasound", in "Encyclopedia of Smart Materials", Ed. M. Schwartz, John Wiley & Sons, New York, 2001, 690-714.
[3] RM .Woodward, BE. Cole, VP. Wallace, RJ. Pye, DD. Arnone, EH. Linfield, M. Pepper “Terahertz pulse imaging in reflection geometry of human skin cancer and skin tissue” : Phys Med Biol. 2002;47, 3853-63.
[4] J. F. Federici, B. Schulkin, F. Huang, D. Gary, R. Barat, F. Oliveira, and D. Zimdars, “THz Imaging and Sensing for Security Applications - Explosives, Weapons, and Drugs”, Semicond. Sci. Technol., 2005, 20, S266-S280
[5] H. Zhong, N. Karpowicz, J. Xu, Y. Deng, W. Ussery, M. Shur, X.-C. Zhang Inspection of Space Shuttle Insulation “Foam Defects Using a 0.2 THz Gunn Diod Oszillator” 12th International Conference on Terahertz Electronics (IEEE Cat. No.04EX857), 2004, 753-7544
[6] T-RAY Diagnostic System, http://www.picometrix.com/t-ray/index.html
[7] W. Hillger, F. Meier, R. Henrich “Inspection of CFRP Components by Ultrasonic Imaging with Air Coupling”, NDT.net, 2002, 7, No.10.
[8] W. Hillger, L. Bühlung, D. Ilse "USPC 4000 AirTech - ein neues, bildgebendes Ultraschallprüfsystem für Ankopplung über Luft", http://www.ndt.net/article/dgzfp04/papers/p09/p09.htm
[9] “Modern Ultrasonic Transducers”, http://www.ultrangroup.com/
[10] T. H. Gan, D. A. Hutchins, D. R. Billson, D. W. Schindel “The use of broadband acoustic transducers and pulse compression techniques for air-coupled ultrasonic imaging”, Ultrasonics, 2001, 39, 181–194.
[11] “EMFIT film specifications”, www.emfit.com
[12] J. Döring, J. Bartusch, A. Erhard, V. Bovtun „Eigenschaften von Polypropylen- und PVDF-Folien für Luftschall-Anwendungen“, DACH - Jahrestagung 2004 Salzburg
[13] J. Döring, W. Stark, J. Bartusch, J. McHugh, W. Simon "Inline-Bestimmung von mechanischen Materialparametern mit einer Ultraschall-Sensorik " to be published in Materialprüfung